

Surface growth during random and irreversible multilayer deposition of straight semirigid rodsN. De La Cruz Félix [†]*Escuela de Física, Instituto de Física (IFIS), Universidad Autónoma de Santo Domingo, Av Alma Mater, Santo Domingo 10105, República Dominicana*P. M. Centres  and A. J. Ramirez-Pastor *Departamento de Física, Instituto de Física Aplicada (INFAP), Universidad Nacional de San Luis–CONICET, Ejército de Los Andes 950, D5700HHW, San Luis, Argentina*S. Bustingorry *Instituto de Nanociencia y Nanotecnología, CNEA-CONICET, Centro Atómico Bariloche, Av. E. Bustillo 9500, R8402AGP San Carlos de Bariloche, Río Negro, Argentina*

(Received 22 April 2021; revised 17 June 2021; accepted 9 August 2021; published 2 September 2021)

Surface growth properties during irreversible multilayer deposition of straight semirigid rods on linear and square lattices have been studied by Monte Carlo simulations and analytical considerations. The filling of the lattice is carried out following a generalized random sequential adsorption mechanism where the depositing objects can be adsorbed on the surface forming multilayers. The results of our simulations show that the roughness evolves in time following two different behaviors: an “homogeneous growth regime” at initial times, where the heights of the columns homogeneously increase, and a “segmented growth regime” at long times, where the adsorbed phase is segmented in actively growing columns and inactive nongrowing sites. Under these conditions, the surface growth generated by the deposition of particles of different sizes is studied. At long times, the roughness of the systems increases linearly with time, with growth exponent $\beta = 1$, at variance with a random deposition of monomers which presents a sublinear behavior ($\beta = 1/2$). The linear behavior is due to the segmented growth process, as we show using a simple analytical model.

DOI: [10.1103/PhysRevE.104.034103](https://doi.org/10.1103/PhysRevE.104.034103)**I. INTRODUCTION**

Deposition is a process of great importance due to its application in the chemical industry and experimentation [1,2]. In statistical mechanics, adsorption models on regular lattices, both in and out of equilibrium, have been useful to study physical adsorption [3–8]. In contrast to reversible adsorption within thermodynamic equilibrium, random sequential adsorption (RSA) models assume that the occupancy state of the lattice sites changes irreversibly from empty to full, providing a useful tool to study irreversible adsorption processes [9–11].

RSA models consists of randomly placing an object on a substrate with the restriction that it does not overlap on previously deposited objects. If a single site changes its occupancy state in an adsorption event from empty to occupied ($0 \rightarrow 1$), then we refer to this as monomer filling. It is also possible to allow pairs of adjacent sites to change ($00 \rightarrow 11$) corresponding to dimer filling, or larger sets of adjacent sites corresponding to k -site filling, in that sense we are talking about an adsorbed k -mer (extended object occupying k adjacent lattice sites) [9]. In most of deposition models, the objects are randomly and irreversibly deposited forming a

single monolayer. The final state generated by RSA is a disordered state (known as jamming state), in which no more objects can be deposited due to the absence of free space of appropriate size and shape. Recent studies show that the size and shape of the deposited objects play an important role in the adsorption kinetics and the final structure of the adsorbed monolayer [12–26].

Most of the studies are devoted to the monolayer adsorption. However, multilayer adsorption is an experimentally as well as theoretically relevant field of surface science owing to its importance for the characterization of solid surfaces [27]. Moreover, several experiments on adhesion of colloidal particles on solid substrates have reported formation of multilayer deposits in essentially irreversible deposition processes from unstable or marginally stable colloid suspensions [28,29].

In the case of irreversible multilayer adsorption, the inherent complexity of the system still represents a major difficulty to the development of approximate and numerical solutions. However, several attempts were done in the past to solve the k -mers irreversible multilayer adsorption problem. Among them, Bartelt and Privman [30] formulated a model of irreversible multilayer adsorption on homogeneous one-dimensional (1D) substrates. In Refs. [31,32], some other variants of the problem were explored: effect of diffusional relaxation, different deposition mechanisms, continuum deposition, etc.

[†]ndelacruz72@uasd.edu.do

Recently, extensive numerical simulations, supplemented by finite-size scaling theory, were used to study the jamming and percolation properties of the irreversible deposition of semirigid k -mers in one and two dimensions [33,34]. In one dimension the formation of multiple layers was allowed [33], and as the k -mer size and number of layers increase, the adsorption process occurs via an in-registry adsorption process, where each incoming k -mer tends to be adsorbed exactly onto an already adsorbed one. The resulting $(1 + 1)$ -dimensional adsorbed phase consists of “towers” (or columns) of width k , separated by valleys of empty sites. In the two-dimensional (2D) case, only two-layers deposition were allowed [34]. The differences between the results obtained from bilayer and monolayer phases were explained on the basis of the transversal overlaps between rods occurring in the bilayer system. This so-called “cross-linking effect,” its consequences on the filling kinetics, and its implications in the field of conductivity of composites filled with elongated particles (or fibers) were discussed in details.

The possibility to form multilayers during the deposition processes opens new opportunities to complement studies which focus in jamming and percolation properties. In particular, a study of the growth properties of the generated surface can shed light on the underlying deposition mechanisms. Interesting quantities to discuss in a multilayer growth model are the surface roughness and growth rate in nonequilibrium conditions, which has attracted considerable interest due to its wide application [35]. Simple and multiple occupational growth models have been studied over 1D and 2D substrates [36–38]. The simplest case is the random deposition (RD) of monomers (k -mers with $k = 1$). Due to the nature of the RD model, the surface grows independently on each site and then the growth properties do not depend on the dimension of the system (it is invariant in one or two dimensions). However, when multiple occupancy occurs the deposition of k consecutive sites generates a correlation between the heights of neighboring columns (the height of each column does not grow independently), which results in compelling growth and roughness properties. Interestingly, while RD of k -mers in 1D can be characterized by a growth exponent, defining how the roughness of the growing surface evolves with time, not depending on the size of the deposited particle [36], RD in 2D shows that the growth exponent depend on the size of the particle [38]. In addition, wetting and rigid cluster deposition models were studied in Ref. [37]. The simulation results show two different behaviors in time, with the initial growth not correlated (as in RD growth) and a subsequent growth presenting a roughness increasing with a growth exponent smaller than in the RD case.

With the aim of complementing the study of surface adsorption of semirigid k -mers, we address here the study of the associated multilayer surface growth process. We present a generalization of the deposition growth model where semirigid rods (k consecutive nearest-neighbor sites) are deposited in multilayers in one and two dimensions. The kinetic growth is studied by dynamic scaling theory and compared with the case of random deposition of monomers. The growth exponent is determined by numerical simulations in one and two dimensions, obtaining a value consistent with a linear increase of the roughness. Using a simple analytical argument we

show that the linear increase of the roughness is due to a fragmentation of the system during the growth process. Our results show that multisite deposition processes can result in nontrivial surface growth properties.

This paper is organized as follows. The multilayer growth model and simulation scheme are presented and discussed in Sec. II. The dynamic growth exponent and correlations in 1D and 2D cases are analyzed in Sec. III. This section includes also the basis of an analytical approach for predicting the growth properties of the studied system, which is presented in Sec. IV. Finally, some conclusions are drawn in Sec. V.

II. MODEL AND BASIC DEFINITIONS

A. Deposition model and simulation scheme

An irreversible multilayer adsorption model in one and two dimensions has been considered. In the 1D system, semirigid k -mers are deposited on a linear lattice of size L . This allows us later to pile up further layers, building up a “wall” of deposited objects, growing in a vertical direction [$(1 + 1)$ -dimensional growth process]. In the 2D system, semirigid k -mers are deposited on a $L \times L$ square substrate leading to a $(2 + 1)$ -dimensional growth process.

As mentioned in the previous paragraph, semirigid k -mers are deposited forming $(1 + 1)$ - and $(2 + 1)$ -dimensional structures. Accordingly, the positions available for adsorption will be indicated by two indices (i, h) . The index i denotes the location in the lattice ($1 \leq i \leq L$ for the 1D case and $1 \leq i \leq L^2$ for the 2D case) and h is the layer number (or height): $h = 1$ for the layer 1 and $h = n$ for the n th layer.

Then, starting from an initially empty lattice, the k -mers are vertically sent toward the surface (similar to a rain of horizontal rods, see Fig. 1). The deposition procedure is carried out following a generalized RSA process [9]. It consists of three steps, namely, (1) one of the ξ possible lattice directions is randomly selected ($\xi = 1$ for the 1D case and $\xi = 2$ for the 2D case); (2) a set of k consecutive nearest-neighbor sites aligned along the direction selected in step (1) is randomly chosen; (3) the deposition attempt will be successful (one k -mer will be deposited) if the difference between the vertical coordinates of two consecutive sites selected in step (2) is at most equal to 1 ($|\Delta h| = 1$ or $|\Delta h| = 0$). Otherwise, the attempt is rejected. One unit time in the deposition procedure in D dimensions corresponds to L^D repetitions of steps (1)–(3). The deposition procedure is performed with periodic boundary conditions, so that all sites are statistically equivalent. Typical configurations obtained by the 1D and 2D deposition schemes are shown in Figs. 1(a) and 1(b), respectively.

According to the deposition rules introduced in the last paragraph (and as shown in Fig. 1): (i) particles do not shrink, so each monomer belonging to a k -mer has its own horizontal coordinate; (ii) particles can partially stretch. Thus, the k -mers can bend to accommodate themselves to the roughness of the interface (substrate and/or previous layers) as far as stretching between consecutive particles does not go over $\sqrt{2}$ interparticle distances, allowing for up to a difference of one vertical position between consecutive monomers belonging to a k -mer; (iii) a k -mer is accepted for deposition only if it is in full contact with the substrate or lower layers without leaving

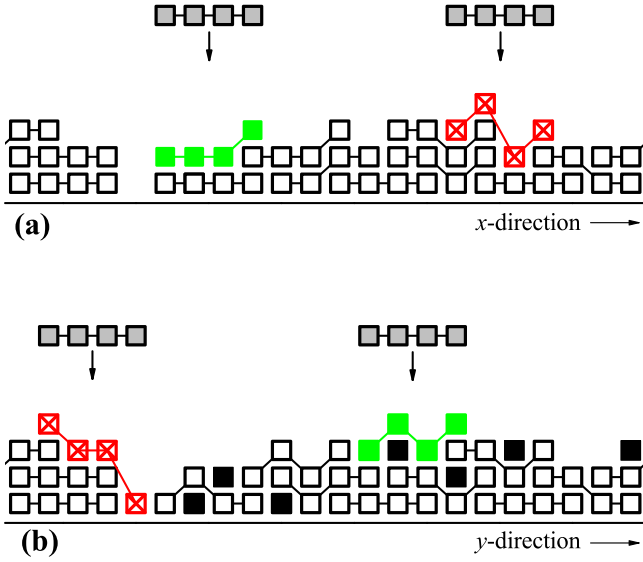


FIG. 1. Schematic representation of tetramers ($k = 4$) deposited (a) on a linear lattice with $L = 22$ and (b) along a line in the y direction of a square lattice with $L = 22$. In both cases, periodic boundary conditions have been applied. As the k -mers are semirigid, they can deform to find adjacent empty sites between layers (but always linear). Open squares joined by lines correspond to tetramers previously deposited onto the lattice. Gray-filled squares joined by lines represent particles attempting to deposit on the substrate. Green-solid squares and red-crossed squares represent allowed and forbidden deposition states, respectively. Forbidden configurations do not satisfy the deposition rules ($|\Delta h| > 1$) and, consequently, are discarded. In panel (b), the units of the transverse k -mers (adsorbed along the x -direction) located at the crossing sites are indicated by black-solid squares.

empty spaces underneath (bridges or cantilevers with two or more empty spaces below are forbidden); and (iv) in the 2D case, although the k -mers are aligned along one of the two axes of the lattice, they can deform to find adjacent empty sites between the first, second, third, fourth..... layer, but always in the same direction. Relaxation is allowed only in the z axis (height) (see Fig. 1).

The main difference between 1D and 2D systems is the occurrence of the “cross-linking effect” in the 2D case. This effect is called as cross-linking effect due the fact that a k -mer adsorbed along the $x[y]$ direction, with one of its units located in a given position $(i, h[h + 1])$ is connected (or linked) to a perpendicular k -mer deposited along the $y[x]$ direction, with one of its units located in the position $(i, h + 1[h])$. The link occurs through the formation of a pair of nearest-neighbor occupied sites in the positions (i, h) and $(i, h + 1)$. Illustrative examples of the occurrence of this “cross-linking effect” are shown in Fig. 1(b). The units of the transversal k -mers located in the crossing sites are indicated by black-solid squares.

B. Kinetic and growth properties

To characterize the growth of a deposited film, it is useful to define the mean height of the multilayer at time t , $\overline{h(t)}$, and

the roughness of the interface at time t , $w(t)$ [35]. Thus,

$$\overline{h(t)} = \frac{1}{L^D} \sum_{i=1}^{L^D} h_i(t), \quad (1)$$

where $h_i(t)$ is the height of the column (at time t) placed in the position i of the lattice and L^D is the total number of sites in each layer on a D -dimensional substrate. In general, the mean height increases linearly with time. In our simulations, the dimensionless MC time variable t is defined by having one deposition attempt per lattice site in the unit time step $\Delta t = 1$. Thus, for a L -lattice, the time step $\Delta t = 1$ corresponds to L^D attempts according to the deposition mechanism described in Sec. II A. Then, time unit is given by the number of attempts η to deposit a particle, $t = \eta/L^D$.

The choice of the time step was done based on previous work by Forgerini and Figueiredo [36,38], which motivated the present study. In this scheme, depending on the size of the particle, many trials of depositions are not successful in the unit of time. Other possible strategies consist in using average height or coverage (amount of mass deposited per unit substrate length) as the time step unit, to remove the dependence on the rate of failures [39]. Since the mean height grows linearly with time, the main results shown below (such as the value of the growth exponent) do not depend on the choice of time step.

The roughness of the interface at time t can be written as

$$w^2(L, t) = \frac{1}{L^D} \sum_{i=1}^{L^D} [h_i(t) - \overline{h(t)}]^2 = \overline{h^2(t)} - \overline{h(t)}^2. \quad (2)$$

The typical behavior of $w(L, t)$ as a function of t is described below. At time zero, the interface is flat and the roughness is nil. As time increases, the interface gradually becomes rough and two different regimes separated by a crossover time t_x can be typically expected: (i) *growth regime*: in which w increases as a power of time according to the power law:

$$w(L, t) \sim t^\beta, \quad \text{for } t \ll t_x, \quad (3)$$

where β is the *growth exponent* that characterizes the growth dynamics and roughness; and (ii) *saturation regime*: during which w reaches a saturation value, w_{sat} , which depends on the lattice size of the system according to the following power law:

$$w_{\text{sat}}(L) \sim L^\alpha \quad \text{for } t \gg t_x, \quad (4)$$

where α is the roughness exponent. The crossover or saturation time t_x also depends on the system size,

$$t_x \sim L^z, \quad (5)$$

where z is the dynamics exponent. The exponents presented in Eqs. (3)–(5) are not independent, α , β , and z being linked by the scaling law:

$$z = \frac{\alpha}{\beta}. \quad (6)$$

The general picture just presented is valid when a correlation length develops in the system, meaning that the height

at one site depends on how the rest of the system is growing. The correlation length increases with time as $t^{1/z}$ and when it reaches the size of the system then the roughness saturates and the roughness exponent α is well defined. In the case of RD model using monomers growing is not correlated and saturation of the roughness is not achieved, with the scaling relation Eq. (6) not applying. Thus, when an interface can grow indefinitely in time, only the growth exponent is defined and in this context the roughness exponent α is not defined, and therefore neither z . Deposition of rigid k -mers induces correlation between growing site [36–38]. However, as we shall see below, the semirigid conditions hinder the growing of the correlation length, segmenting the system in sections characterized by RD growth.

As discussed in Sec. I, the formation of multilayers during a deposition process can be also analyzed in terms of the coverage $\theta(t)$, defined as the ratio of the total number of occupied lattice sites at time t with respect to the total number of available sites (the total number of available sites is given by $n_t L^D$, where n_t is the total number of layers forming the multilayer at time t). By comparing the definitions of mean height $\bar{h}(t)$ and coverage $\theta(t)$, it is straightforward that $\theta(t) = \bar{h}(t)/h_{\max}$, where h_{\max} is the maximum height (or total number of layers $n_t = h_{\max}$). For the rest of the paper, we will focus our attention on the time-dependent roughness and associated quantities.

III. MONTE CARLO SIMULATIONS RESULTS

The complexity of the irreversible multilayer adsorption problem presents a major difficulty to the development of accurate analytical solutions for $\bar{h}(t)$ and $w(t)$. So, computer simulations appear as a very important tool for investigating this subject, and will be used in the present section.

We focus our calculations on the estimate of the scaling exponents for 1D and 2D substrates. For this purpose, extensive computer simulations were developed for $k = 1, 2, 3, 4, 6, 8, 12, 16$ and different lattice sizes: 1D lattices with $L = 1024, 2048, 3072, 4096, 5120$; and 2D $L \times L$ square lattices with $L = 96, 192, 384, 512, 576, 768$. In all cases, the displayed results represent averages considering 10^5 different samples.

From the numerical simulations, the mean height as a function of time, $\bar{h}(t)$, increases linearly with time, regardless of the value of k and the dimensionality considered (these curves are not shown for simplicity). Next, the surface roughness as a function of time was studied. Typical curves of $w(t)$ are shown in Fig. 2 (in log-log scale). The results correspond to 1D lattices with $L = 5120$ [Fig. 2(a)] and 2D lattices with $L = 512$ [Fig. 2(b)] for different values of k as indicated. In the case of $k = 1$ (solid squares), the expected behavior for the RD model is found: $\beta = 1/2$ in any spatial dimension and no saturation regime is observed [35]. The situation changes drastically for $k \geq 2$, where the roughness varies in time following two different regimes. At the initial times, the growth exhibits a transitory nonlinear behavior. Then, at long times, the interface roughness grows faster, with another growth exponent $\beta \approx 1$, which is not in the same universality class of the $k = 1$ RD model. In addition, no saturation regime

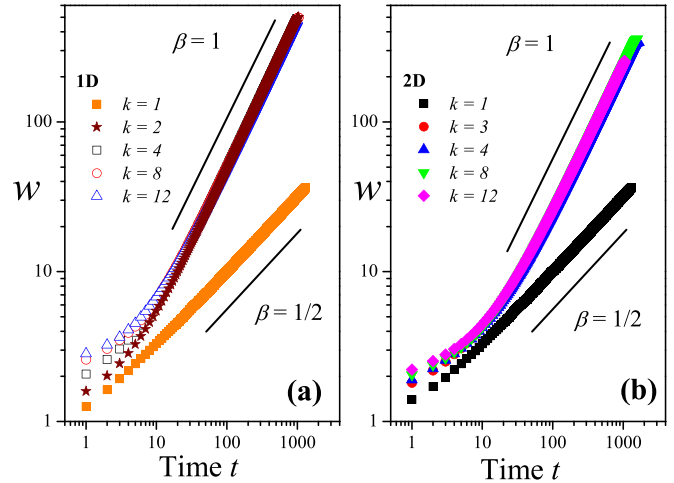


FIG. 2. Surface roughness as a function of time (in log-log scale) for 1D lattices with $L = 5120$ [panel (a)] and 2D lattices with $L = 512$ [panel (b)]. The different curves correspond to different values of k , as indicated in the key. The growth exponent keeps consistency with the case of RD monomers, whose exact solution is ($\beta = 1/2$) [35]. Two growth regimes are observed for $k \geq 2$, with $\beta = 1$ the growth exponent for long times.

is reached for $k \geq 2$ and, accordingly, the exponent α is not defined.

The procedure in Fig. 2 was repeated for all values of L and k . The obtained values of β are compiled in Table I (second column, 1D system; third column, 2D system). For each k , the value informed of β represents an average over all the studied lattice sizes in one and two dimensions. The phenomenology is identical comparing the 1D and 2D cases.

The two regimes characterizing the growth rate of the surface can be explained as follows. Once the growth process begins, the occupancy of the sites increases with a homogeneous probability, but after a certain time, the greatest probability of sticking is over the previously deposited k -mers. Then, while some columns grow, other columns stop growing due to not satisfying the condition $|\Delta h| \leq 1$ (see Sec. II A). Thus, at long times, the resulting structure of the adsorbed phase consists of columns of width k , separated by valleys of empty sites.

TABLE I. The growth exponents for different rods sizes in one and two-dimensional lattices. For each k , the value informed of β represents an average over all studied lattice sizes: $L = 1024, 2048, 3072, 4096, 5120$ (1D system); and $L = 96, 192, 384, 512, 576, 768$ (2D system).

k size	β (1D system)	β (2D system)
1	0.50 ± 0.01	0.49 ± 0.02
2	1.00 ± 0.01	0.98 ± 0.02
3	1.00 ± 0.01	0.99 ± 0.02
4	0.99 ± 0.02	0.99 ± 0.02
6	0.99 ± 0.02	0.99 ± 0.02
8	1.00 ± 0.02	0.99 ± 0.02
12	0.99 ± 0.02	0.99 ± 0.02
16	0.99 ± 0.02	0.99 ± 0.02

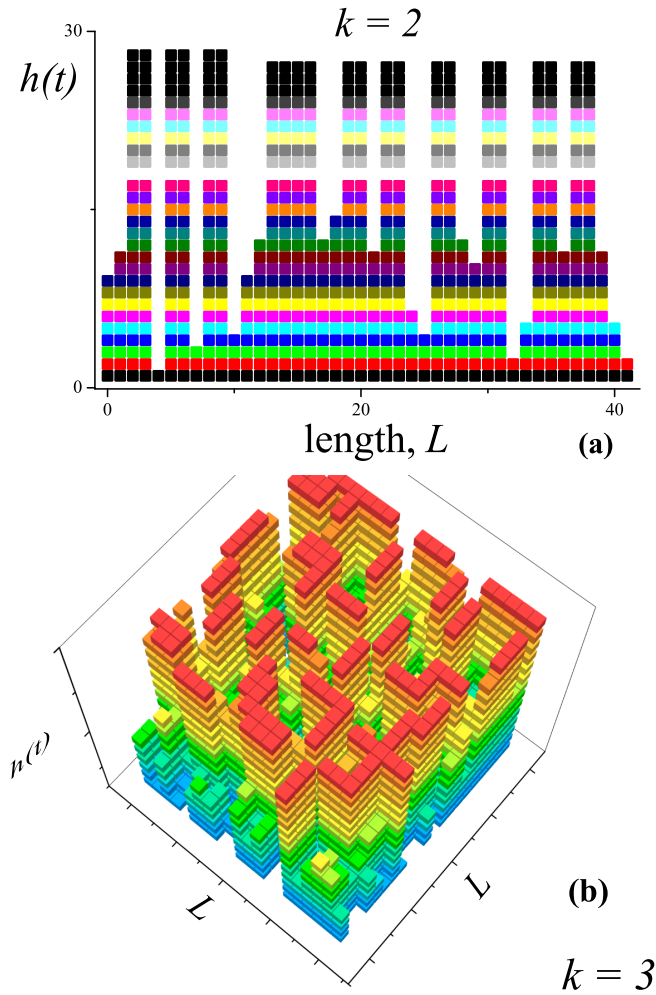


FIG. 3. Typical configurations of the adsorbed phase in the SGR. Two cases are shown in the figure: (a) 1D system with $k = 2$; and (b) 2D system with $k = 3$. Solid squares [panel (a)] and solid cubes [panel (b)] represent k -mer units. As time t increases, the k -mer units tend to form islands of length k in each layer.

We call the first regime (at initial time) as “homogeneous growth regime” (HGR), due to the homogeneous increase in the height of the columns. However, we call the second regime (at long times) as “segmented growth regime” (SGR), since the adsorbed phase is segmented in growing and not-growing columns. These concepts will be reviewed in detail in the next section.

To illustrate the behavior of the system at long times, Fig. 3 shows two typical configurations of the adsorbed phase in the SGR. Figure 3(a) corresponds to 1D system with $k = 2$, and Fig. 3(b) corresponds to 2D system with $k = 3$. As it can be observed from the figures, k -mers in the n th layer adsorb in-registry with the adsorbed k -mers in the $(n - 1)$ th layer, forming columns of width k separated by low columns (whose difference in height with neighboring columns is greater than one, $|\Delta h| \geq 1$). These findings demonstrate that the relaxation condition $|\Delta h| \geq 1$ is the cause of the segmentation observed in the system.

To characterize the state of the system in the SGR, let us consider that the entire adsorbed phase can be studied as a

set of overlapping linear lattices, each one corresponding to one of the n layers [41]. Then, the Hoshen and Kopelman algorithm [40] has been used to obtain the number of islands of length λ in each layer. The occurrence frequency of an island of size λ in the n th layer is denoted as $f_n(\lambda)$, where $f_n(\lambda)$ is the ratio between the total number of islands of size λ in the n th layer and the total number of islands in the n th layer. The coverage in the n th layer θ_n was also calculated. θ_n is defined as the ratio between the number of occupied sites on the n th layer and the total number of sites in each layer (L^D).

The analysis of $f_n(\lambda)$ for different values of k shows that, for relatively small values of n ($4 \lesssim n \lesssim 8$), the structure of the adsorption state is mainly composed of islands of sizes k and $2k$. As n is increased ($n \gtrsim 8$), islands of size k dominate the adsorption state. The effect is even more marked as the size k is increased. In the case of the coverage in the n th layer for large n (long times), θ_n increases with increasing k and, accordingly, the space of empty sites in the n th layer diminishes with k . The results obtained for $f_n(\lambda)$ and θ_n indicate that only columns of width k “survives” in the SGR. These columns are separated by valleys of empty sites. As k increases, the separation distance between columns diminishes. This general phenomenology associated with the SGR is also captured by the mean towers density, as we will show in the next section.

The occurrence of two growth regimes has already been reported for RD of linear objects of different lengths on 1D [36] and 2D [38] substrates. In these cases a fully rigid object is deposited if around a randomly selected site, corresponding to the midpoint of the linear object, there is enough horizontal space to accommodate it. This mechanism, at variance with our model, generates voids in the growing surface. In contrast with the present data, a saturation regime is observed in Refs. [36,38]. The saturation regime is also found in Ref. [37] for the case of fully flexible clusters of particles deposited in a 1D lattice. In this case the linear cluster adapts its form to the surface at a random place, without leaving empty spaces and generating a compact surface growth.

The results presented here complement previous works [36–38], showing how the segmentation of the interface causes the surface roughness to not saturate and grow indefinitely with time, but with a growth exponent different to the one corresponding to the monomer RD model. Our model exhibits a short-time regime with a nonlinear growth followed by linear roughness growth with an exponent $\beta = 1$, independently of the dimensionality of the system. The results in Refs. [36,38] show a typical RD behavior with an exponent $\beta_1 = 0.5$ at short-times followed by a growth exponent $\beta_2 < 0.5$ in the 1D case [36] and a $\beta_2 > 0.5$ in the 2D case [38]. In addition, while the exponents β we found here and β_2 in Ref. [36] remain constant no matter the size of the objects used in the simulations, the exponent β_2 in Ref. [38] shows a nonuniversal behavior, being strongly dependent on the particle size.

In the next section, an analytical approach is set up to describe the evolution of the roughness as a function of time. This approximation will allow us to better understand the behavior of the system, and the main characteristics of the SGR.

IV. THEORETICAL MODEL FOR THE SURFACE ROUGHNESS

Hereafter, we present a theoretical analysis that sheds light on the underlying physics of the observed time dependence of the surface roughness $w(t)$. We first briefly derive the time-evolution of the roughness for the random deposition of monomers, which permit us to describe the procedure we use to later obtain the roughness for the segmented growth regime.

Let us start with the case of classical RD of monomers ($k = 1$). A discrete system of finite size L^D is considered in which each site grows independently. The probability that a particle will be deposited at the i site is $p = 1/L^D$. As introduced in Sec. II B, the unit of time is given by the number of attempts η to deposit a particle, $t = \eta/L^D$. The probability that the height of the i site is h_i after η attempts is

$$P(h_i, \eta) = \binom{\eta}{h_i} p^{h_i} (1-p)^{\eta-h_i}, \quad 0 \leq h_i \leq \eta, \quad (7)$$

with mean value $\langle h_i \rangle = \eta p$ and mean-squared value $\langle h_i^2 \rangle = \eta p(1-p) + \eta^2 p^2$. In addition, since the growth is independent on each site, it results that $\overline{h(t)} = \langle h_i(t) \rangle$ and $\overline{h^2(t)} = \langle h_i^2(t) \rangle$. Finally, by using Eq. (2), the surface roughness can be written as

$$\begin{aligned} w^2(L, t) &= \overline{h^2(t)} - \overline{h(t)}^2 = \langle h_i^2(t) \rangle - \langle h_i(t) \rangle^2 \\ &= \eta p(1-p) = t \left(1 - \frac{1}{L^D} \right). \end{aligned} \quad (8)$$

For large systems ($L \rightarrow \infty$), $w^2 = t$ and the growth exponent is $\beta = 1/2$.

Let us now consider the case of k -mers deposited in a D -dimensional lattice of linear size L in the SGR, i.e., when the system is segmented and independently growing on each tower. Under these conditions, the system is segmented into active sites and inactive sites. Neglecting cross-linking effects in the SGR, the active sites are those that make up the towers of size k , where growth can continue (because the depositing objects are k -mers). If there are m towers, then there are km active sites. We call \mathcal{A} the set of active sites. In the inactive sites it is no longer possible to grow (in the SGR) and the average height of the inactive sites will be saturated. The probability that a k -mer will be deposited with one end at the i site is $p = (\xi L^D)^{-1}$. Note that in the particular case of linear and square lattices $\xi = D$. It is important to remark that the difference in height between two nearest-neighbor active sites is $\Delta h \leq 1$. Thus, the active sites do not necessarily belong to the same layer.

If we define the l th tower (with $l = 1, 2, \dots, m$) as the one that occupies the sites $i, i+1, \dots, i+k-1$, and since the individual towers grow independently of each other, then it results (as in the case of $k = 1$): $\langle h_l \rangle = \eta p$ and $\langle h_l^2 \rangle = \eta p(1-p) + \eta^2 p^2$, where h_l is the height of all the columns in the l th tower. In addition, we consider that the height is constant and equal to h_{in} for all inactive sites.

In the SGR, the mean height of the system will be

$$\overline{h(t)} = \frac{1}{L^D} \left[\sum_{i \in \mathcal{A}} h_i(t) + \sum_{i \notin \mathcal{A}} h_{\text{in}} \right]. \quad (9)$$

Considering that the towers grow independently, and that all sites in the same tower grow simultaneously, we can write $h_i(t) = \langle h_l(t) \rangle$ for the active sites in tower l and $h_i(t) = h_{\text{in}}$ for the inactive sites. Thus,

$$\begin{aligned} \overline{h(t)} &= \frac{1}{L^D} \left[\sum_{i \in \mathcal{A}} \langle h_l(t) \rangle + \sum_{i \notin \mathcal{A}} h_{\text{in}} \right] \\ &= \frac{mk}{L^D} \langle h_l(t) \rangle + \frac{(L^D - mk)}{L^D} h_{\text{in}}. \end{aligned} \quad (10)$$

Now, by using $\langle h_l \rangle = \eta p$ and by defining $\theta_a = mk/L^D$ as the fraction of active sites, Eq. (10) can be written as

$$\overline{h(t)} = \theta_a \eta p + (1 - \theta_a) h_{\text{in}}. \quad (11)$$

In the same way,

$$\begin{aligned} \overline{h^2(t)} &= \frac{1}{L^D} \left[\sum_{i \in \mathcal{A}} h_i^2(t) + \sum_{i \notin \mathcal{A}} h_{\text{in}}^2(t) \right] \\ &= \frac{1}{L^D} \left[\sum_{i \in \mathcal{A}} \langle h_l^2(t) \rangle + \sum_{i \notin \mathcal{A}} h_{\text{in}}^2 \right] \\ &= \theta_a [\eta p(1-p) + \eta^2 p^2] + (1 - \theta_a) h_{\text{in}}^2. \end{aligned} \quad (12)$$

By using Eqs. (11), (12), and $p = (\xi L^D)^{-1}$, we can write the surface roughness as a function of time $t = \eta/L^D$ as:

$$\begin{aligned} w^2(L, t) &= \overline{h^2(t)} - \overline{h(t)}^2 = \theta_a(1 - \theta_a) \left(\frac{t}{\xi} - h_{\text{in}} \right)^2 \\ &\quad + \theta_a \left(1 - \frac{1}{\xi L^D} \right) \frac{t}{\xi}. \end{aligned} \quad (13)$$

For large systems ($L \rightarrow \infty$), long times ($t \rightarrow \infty$) and because $\theta_a < 1$ in the SGR, Eq. (13) reduces to $w^2 = \theta_a(1 - \theta_a)t^2/\xi^2$. Accordingly, $\beta = 1$ as obtained by MC simulations. The terms proportional to $(\eta p)^2$ are not canceled in the SGR and therefore the trend t^2 survives. In other words, the value of the growth exponent $\beta = 1$ is the result of the segmentation of the adsorbed phase. Note that, if $\theta_a = 1$, then the case $k = 1$ (classical RD of monomers) is recovered, where $w^2 = (1 - 1/L^D)t$ and $\beta = 1/2$.

It is interesting to extend the analysis of Eq. (13) in the limit of $t \rightarrow \infty$, namely,

$$\log w(t) = \frac{1}{2} \log[\theta_a(1 - \theta_a)] - \log \xi + \log t = \rho + \beta \log t, \quad (14)$$

where $\beta = 1$ and

$$\rho = \frac{1}{2} \log[\theta_a(1 - \theta_a)] - \log \xi = \frac{1}{2} \log \Omega_a - \log \xi, \quad (15)$$

where $\Omega_a = \theta_a(1 - \theta_a)$. The parameter ρ is of practical interest because it represents the intercept of the log-log relationship between surface roughness w and time t in the long-time limit.

The theoretical predictions from Eq. (14) can be corroborated with the help of the simulation data in Fig. 2. Thus, for $k > 1$ and fixed ξ (in our case, $\xi = 1$ for 1D lattices and $\xi = 2$ for 2D square lattices), the value of ρ does not depend on the particle size k . Independently of the size k , all 1D(2D) curves

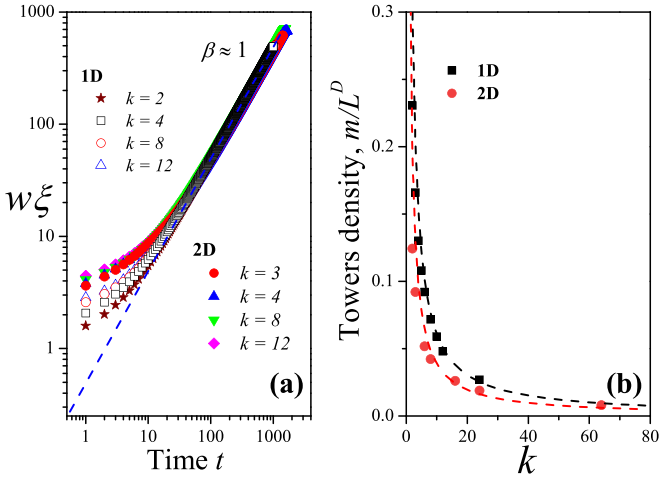


FIG. 4. (a) Time dependence of the scaled roughness $w\xi$. In the long-time limit, 1D and 2D results collapse to the same linear behavior in logarithmic scale. The dashed line corresponds to $1/2 \log \tilde{\Omega}_a + \log t$, where $\tilde{\Omega}_a = 0.238$. (b) Towers density m/L^D as a function of k for 1D and 2D lattices. Symbols represent simulation data with $L = 5120$ (1D case, solid squares) and $L = 512$ (2D case, solid circles). Dashed lines correspond to the functions $\theta_{a,1D}/k$ (1D case, $\theta_{a,1D} = 0.61$) and $\theta_{a,2D}/k$ (2D case, $\theta_{a,2D} = 0.39$). The results confirm the analytically predicted values of the fraction of active sites.

collapse in a unique curve in the SGR [all 1D(2D) curves have the same intercept ρ on the vertical axis]. See Figs. 2(a) and 2(b).

However, and as can be seen from Eq. (15), the value of ρ depends on the dimensionality of the system through the number of possible lattice directions ξ and the fraction of active sites θ_a . The values of ρ can be obtained by fitting the long-time regimes in Fig. 2, resulting in $\rho_{1D} = -0.311 \pm 0.002$ (1D system, $\xi = 1$) and $\rho_{2D} = -0.614 \pm 0.003$ (2D system, $\xi = 2$).

From Eq. (15), we can write that

$$\rho_{1D} - \rho_{2D} = \frac{1}{2} \log \left(\frac{\Omega_{a,1D}}{\Omega_{a,2D}} \right) + \log 2. \quad (16)$$

Then, by using the measured values of ρ_{1D} and ρ_{2D} in Fig. 2, we get that $\rho_{1D} - \rho_{2D} = 0.303 \pm 0.005$, which is consistent, within statistical errors, with $\rho_{2D} - \rho_{1D} = \log 2 = 0.30102999 \dots$. This finding indicates that: (1) $\Omega_{a,1D} \approx \Omega_{a,2D}$, meaning that Ω_a does not depend on the dimension of the substrate [from Figs. 2(a) and 2(b), we obtain $\Omega_{a,1D} = 0.239 \pm 0.001$ and $\Omega_{a,2D} = 0.237 \pm 0.003$, respectively]; and (2) the relation between the fractions of active sites in 1D and 2D is either $\theta_{a,1D} = \theta_{a,2D}$ or $\theta_{a,1D} = 1 - \theta_{a,2D}$.

The results discussed in the last paragraph are confirmed in Fig. 4. In Fig. 4(a), 1D and 2D simulation data collapse in the SGR by plotting the scaled roughness $w\xi$ against t . The curves grow linearly in logarithmic scale, $\log(w\xi) = 1/2 \log \Omega_a + \log t$, with the same ordinate value. The dashed line in the figure corresponds to $1/2 \log \tilde{\Omega}_a + \log t$, where $\tilde{\Omega}_a = (\Omega_{a,1D} + \Omega_{a,2D})/2 = 0.238 \pm 0.002$. The value of the concentration of active sites θ_a can be calculated from the obtained value of $\tilde{\Omega}_a$ using $\theta_a(1 - \theta_a) = \tilde{\Omega}_a$ [see Eq. (15)].

The equation has two solutions, with $\theta_{a1} = 0.39 \pm 0.01$ and $\theta_{a2} = 0.61 \pm 0.01$, where $\theta_{a1} + \theta_{a2} = 1$.

The obtained values for the fraction of active sites, θ_{a1} and θ_{a2} , are based on the value of $\tilde{\Omega}_a$, which depends on measured values of ρ_{1D} and ρ_{2D} . Therefore, θ_{a1} and θ_{a2} were obtained in terms of information coming from the dynamics of the underlying growth process. We can compare this result with a static measure of the tower density at very long times, $m/L^D = \theta_a/k$, which should decrease when k increases. Figure 4(b) shows this trend for one and two dimensions, directly measuring m/L^D from MC results at long times. Simulation data (solid symbols) are compared with analytical curves (dashed lines) for 1D case ($\theta_{a,1D}/k$ with $\theta_{a,1D} = 0.61$) and 2D case ($\theta_{a,2D}/k$ with $\theta_{a,2D} = 0.39$). A good agreement is obtained between MC and theoretical results, validating the methodology developed in this section.

The analytical description presented here provides a simple basis to interpret the numerical results. It shows how the segmentation of the system in active and inactive growing regions is responsible of the $\beta = 1$ behavior at long times and without presenting a saturation of the roughness. Besides, simple arguments quantitatively relate the measured ρ values with the tower density at long times.

V. CONCLUSIONS

In this paper, a surface growth model has been studied, where semirigid linear objects (k -mers) of different sizes are deposited on linear (1D) and square (2D) lattices. The main deposition rules are the following: (i) the particles are deposited parallel to the substrate, so each monomer belonging to a k -mer has its own horizontal coordinate; (ii) the k -mers can bend to accommodate themselves to the roughness of the interface, allowing for up to a difference of one vertical position between consecutive monomers belonging to a k -mer; and (iii) the k -mers are deposited in full contact with the substrate or lower layers without leaving empty spaces underneath.

By means of Monte Carlo simulations, the evolution of the surface roughness with time was investigated. In the case of $k = 1$ (monomers), the expected behavior for the RD model is found: $w(t) \propto t^\beta$ with $\beta = 1/2$ in any spatial dimension, and no saturation regime is observed [35].

The phenomenology changes drastically for multisite deposition ($k \geq 2$), where the roughness varies in time following two different regimes. At the initial times, the growth exhibits a transitory nonlinear behavior, characterized by a homogeneous increase in the height of the columns. This first regime was called as ‘‘homogeneous growth regime’’ (HGR). Then, at long times, the greatest probability of sticking is over the previously deposited k -mers. Under these conditions, due to the semirigid character of the k -mers, while some columns grow, other columns stop growing due to not satisfying the condition $|\Delta h| \leq 1$. The resulting structure of the interface is segmented in growing (or active) columns of width k , separated by valleys of not-growing columns. In this second regime [called as ‘‘segmented growth regime’’ (SGR)], the surface roughness exhibits a linear dependence on time, with a growth exponent $\beta = 1$, which is not in the same universality class of the $k = 1$ RD model. The long-time behavior, $w(t) \propto t$, is found

to be independent of k -mer size and dimensionality of the substrate.

In addition, and as a consequence of the segmentation that occurs in the adsorbed phase, the active columns grow independently of each other and the surface roughness does not saturate and grows indefinitely with time. This finding contrasts with previous studies on growth by deposition of k -mers, where a saturation regime is reached [36–38]. With respect to the time evolution of surface roughness, two regimes were also found in Refs. [36,38]. However, there are some differences between the results presented here and those in Refs. [36,38]. Namely, while our model exhibits a nonlinear growth at the initial stage, Refs. [36,38] show a typical RD behavior with an exponent $\beta_1 = 0.5$. In the second regime, while in our model the surface roughness grows with an exponent $\beta = 1$, independently of the particle size ($k \geq 2$) and dimensionality of the system, a growth exponent $\beta_2 < 0.5$ was found in 1D [36] and a $\beta_2 > 0.5$ in 2D [38]. In the case of 2D square lattices, the exponent $\beta_2 > 0.5$ is nonuniversal, depending on the length of the deposited particles [38]. These differences are due to the semirigid quality of the deposited k -mers, which was not considered in Refs. [36–38].

Finally, a simple analytical model was proposed to describe the dependence of the surface roughness on time in the SGR, where $\log w(t) = \rho + \beta \log t$, with $\beta = 1$. The theoretical predictions corroborate the numerical results, also showing that the exponent $\beta = 1$ and the absence of a saturation regime can be explained from the segmentation of the system in active and inactive growing regions. In addition, the analytical expression obtained for $w(t)$ allows for a simple relationship between the measured intercept ρ and the fraction of active sites θ_a (size of the active growing region).

ACKNOWLEDGMENTS

This work was supported in part by CONICET (Argentina) under Project No. PIP112-201101-00615; Universidad Nacional de San Luis (Argentina) under Project No. 03-0816; Ministry of Higher Education, Science and Technology, MESCYT-Dominican Republic under Project No. FONDOCYT-2016-2017-084 and OAS Academic Scholarship Program (Graduate). The numerical work was done using the BACO parallel cluster located at Instituto de Física Aplicada, Universidad Nacional de San Luis–CONICET, San Luis, Argentina.

-
- [1] N. S. Samarasingha, S. Zollner, D. Pal, R. Singh, and S. Chattopadhyay, *J. Vacuum Sci. Technol. B* **38**, 042201 (2020).
- [2] T. Xie, C. Licai, Z. Xiaolan, Y. Jiajun, L. Wulin, and D. Zhou, *Thin Solid Films* **705**, 138037 (2020).
- [3] S. Brunauer, P. H. Emmett, and E. Teller, *J. Am. Chem. Soc.* **60**, 309 (1938).
- [4] G. Halsey, *J. Chem. Phys.* **16**, 931 (1948).
- [5] T. L. Hill, *Adv. Catal.* **4**, 211 (1952).
- [6] S. B. Casal, H. S. Wio, and S. Mangioni, *Physica A* **311**, 443 (2002).
- [7] F. Romá, A. J. Ramirez-Pastor, and J. L. Riccardo, *Surf. Sci.* **583**, 213 (2005).
- [8] F. O. Sánchez-Varretti, G. D. García, A. J. Ramirez-Pastor, and F. Romá, *J. Chem. Phys.* **130**, 194711 (2009).
- [9] J. W. Evans, *Rev. Mod. Phys.* **65**, 1281 (1993).
- [10] A. Cadilhe, N. A. M. Araújo, and V. Privman, *J. Phys.: Condens. Matter* **19**, 065124 (2007).
- [11] N. A. M. Araújo and A. Cadilhe, *J. Stat. Mech.* (2010) P02019.
- [12] P. L. Krapivsky, S. Redner, and E. Ben-Naim, *A Kinetic View of Statistical Physics* (Cambridge University Press, Cambridge, UK, 2010).
- [13] G. Kondrat, Z. Koza, and P. Brzeski, *Phys. Rev. E* **96**, 022154 (2017).
- [14] M. G. Slutski, L. Y. Barash, and Y. Y. Tarasevich, *Phys. Rev. E* **98**, 062130 (2018).
- [15] M. Pawłowska and A. Sikorski, *J. Mol. Model.* **19**, 4251 (2013).
- [16] M. Nakamura, *J. Phys. A* **19**, 2345 (1986).
- [17] B. J. Brosilow, R. M. Ziff, and R. D. Vigil, *Phys. Rev. A* **43**, 631 (1991).
- [18] V. Privman, J.-S. Wang, and P. Nielaba, *Phys. Rev. B* **43**, 3366 (1991).
- [19] I. A. Kriuchevskiy, L. A. Bulavin, Y. Y. Tarasevich, and N. I. Lebovka, *Condens. Matter Phys.* **17**, 33006 (2014).
- [20] A. J. Ramirez-Pastor, P. M. Centres, E. E. Vogel, and J. F. Valdés, *Phys. Rev. E* **99**, 042131 (2019).
- [21] R. D. Vigil and R. M. Ziff, *J. Chem. Phys.* **93**, 8270 (1990).
- [22] R. Dickman, J.-S. Wang, and I. Jensen, *J. Chem. Phys.* **94**, 8252 (1991).
- [23] M. Cieřła and J. Barbasz, *Phys. Rev. E* **90**, 022402 (2014).
- [24] M. Cieřła and P. Karbownik, *Phys. Rev. E* **91**, 042404 (2015).
- [25] M. Cieřła, G. Pająk, and R. M. Ziff, *Phys. Chem. Chem. Phys.* **17**, 24376 (2015).
- [26] M. Cieřła, G. Pająk, and R. M. Ziff, *J. Chem. Phys.* **145**, 044708 (2016).
- [27] S. J. Gregg and K. S. W. Sing, *Adsorption, Surface Area, and Porosity* (Academic Press, New York, 1991).
- [28] N. Ryde, N. Kallay, and E. Matijević, *J. Chem. Soc. Faraday Trans.* **87**, 1377 (1991).
- [29] N. Kallay, M. Tomić, B. Biškup, I. Kunjašić, and E. Matijević, *Colloids Surf.* **28**, 185 (1987).
- [30] M. C. Bartelt and V. Privman, *J. Chem. Phys.* **93**, 6820 (1990).
- [31] V. Privman and J.-S. Wang, *Phys. Rev. A* **45**, R2155 (1992).
- [32] P. Nielaba, V. Privman, and J.-S. Wang, *Berich. Bunsen. Gesell.* **98**, 451 (1994).
- [33] N. De La Cruz Félix, P. M. Centres, A. J. Ramirez-Pastor, E. E. Vogel, and J. F. Valdés, *Phys. Rev. E* **102**, 012106 (2020).
- [34] N. De La Cruz Félix, P. M. Centres, and A. J. Ramirez-Pastor, *Phys. Rev. E* **102**, 012153 (2020).
- [35] A.-L. Barabási and H. E. Stanley, *Fractal Concepts in Surface Growth* (Cambridge University Press, Cambridge, UK, 1995).

- [36] F. L. Forgerini and W. Figueiredo, *Phys. Rev. E* **79**, 041602 (2009).
- [37] D. A. Mirabella and C. M. Aldao, *Surf. Sci.* **646**, 282 (2016).
- [38] F. L. Forgerini and W. Figueiredo, *Phys. Rev. E* **81**, 051603 (2010).
- [39] N. Provatas, M. Haataja, J. Asikainen, S. Majaniemi, M. Alava, and T. Ala-Nissila, *Colloids and Surfaces A: Physicochem. Eng. Aspects* **165**, 209 (2000).
- [40] J. Hoshen and R. Kopelman, *Phys. Rev. B* **14**, 3438 (1976).
- [41] We restrict to the 1D case to facilitate the analysis. Similar results are obtained for 2D substrates.